^{11}B NMR: A New Tool for the Determination of Hapticity of Tris(pyrazolyl)borate Ligands

Todd O. Northcutt, Rene J. Lachicotte, and William D. Jones*

Department of Chemistry, University of Rochester, Rochester, New York 14627

Received July 6, 1998

While X-ray crystallography provides reliable solid-state information, the assignment of hapticity in [HB(3,5-dimethylpyrazolyl)$_3$]ML$_n$ (M = Rh, Ir, Pt) complexes in solution is complicated by the dynamic nature of the tris(pyrazolyl)borate ligand. ^{1}H and ^{13}C NMR spectroscopy is ambiguous as to the nature of the coordination environment around the metal center. ^{11}B NMR data are shown to correlate with the hapticity of the tris(pyrazolyl)borate ligand, making it a useful tool for the rapid determination of solution-state structure of tris(pyrazolyl)borate metal complexes.

Introduction

In recent years the use of tris(pyrazolyl)borate ligands has seen marked growth.[1] Though often referred to as cyclopentadienyl analogues, tris(pyrazolyl)borate ligands can exhibit more complex coordination behavior with both η^2 and η^3 binding modes being accessible. In particular, complexes of the type Tp^{R}ML$_2$ (L = CO, olefin, isocyanide, phosphine) display this hapticity ambiguity, with the binding mode of the pyrazolylborate ligand dependent upon the nature of R, M, and L. When this ligand is bound in the η^2 fashion, a 16-electron square-planar species results, while η^3 coordination yields an 18-electron trigonal-bipyramidal structure. The hapticity of the ligand can have a dramatic effect on the reactivity of the complex. For example, the incorporation of ^{13}CO into Tp^{Ph}Rh(CO)$_2$, which exists as a mixture of η^2 and η^3 isomers in solution (85:15), is complete within 5 min. Tp*Rh(CO)$_2$, in which the pyrazolylborate ligand is bound solely in the η^3 fashion, does not incorporate the label over the course of 4 h, as there is no open site for associative substitution.[2]

Though reliable solid-state coordination information is provided by X-ray crystallography, the assignment of hapticity in Tp^{R}ML$_2$ complexes in solution is complicated by the dynamic nature of the tris(pyrazolyl)borate ligand. In both ^{1}H and ^{13}C NMR spectra, static square-planar and trigonal-bipyramidal structures would be expected to show a 2:1 pattern of pyrazolyl resonances. However, many Tp^{R}ML$_2$ complexes display only a single set of pyrazolyl resonances even at low temperatures.[3−21] The equilibration of pyrazolyl rings is consistent with the rapid exchange of coordinated and uncoordinated rings (eq 1).

It should be noted that only the equatorial pyrazolyl rings are exchanged by this mechanism. Thus, in Tp^{R}MLL′ complexes a 2:1 pattern of pyrazolyl resonances is observed.[22−29] If both equatorial and axial pyrazolyl rings were involved in the exchange mechanism (e.g. Berry pseudoroataion), only a single set of pyrazolyl resonances would be observed.

(1) Trofimenko, S. *Chem. Rev.* **1993**, *93*, 943−980. Kitakima, N.; Tolman, W. B. *Prog. Inorg. Chem.* **1995**, *43*, 419−531.
(2) Krentz, R. Ph.D. Thesis, University of Alberta, Edmonton, AB, Canada, 1989.
(3) Trofimenko, S. *J. Am. Chem. Soc.* **1969**, *91*, 588−595.
(4) O'Sullivan, D. J.; Lalor, F. J. *J. Organomet. Chem.* **1974**, *65*, C47−C49.
(5) Cocivera, M.; Ferguson, G.; Lalor, F. J.; Szczecinski, P. *Organometallics* **1982**, *1*, 1139−1142.
(6) Ghosh, C. K.; Graham, W. A. G. *J. Am. Chem. Soc.* **1987**, *109*, 4726−4727.
(7) Tanke, R. S.; Crabtree, R. H. *Inorg. Chem.* **1989**, *28*, 3444−3447.
(8) Jones, W. D.; Hessell, E. T. *Inorg. Chem.* **1991**, *30*, 778−783.
(9) Fernandez, M. J.; Rodriguez, M. J.; Oro, L. A. *Polyhedron* **1991**, *10*, 1595−1598.
(10) Bovens, M.; Gerfin, T.; Gramlich, V.; Petter, W.; Venanzi, L. M.; Haward, M. T.; Jackson, S. A.; Eisenstein, O. *New J. Chem.* **1992**, *16*, 337−345.
(11) Rheingold, A. L.; White, C. B.; Trofimenko, S. *Inorg. Chem.* **1993**, *32*, 3471−3477.
(12) Ciriano, M. A.; Fernández, J. M.; Rodríguez, M. J.; Oro, L. A. *Organomet. Chem.* **1993**, *443*, 249−252.
(13) Rheingold, A. L.; Ostrander, R. L.; Haggerty, B. S.; Trofimenko, S. *Inorg. Chem.* **1994**, *33*, 3666−3676.
(14) Pérez, P. J.; Poveda, M. L.; Carmona, E. *Angew. Chem., Int. Ed. Engl.* **1995**, *34*, 231−233.
(15) Bucher, U. E.; Fässler, T. F.; Hunziker, M.; Nesper, R.; Rüegger, H.; Venazi, L. M. *Gazz. Chim. Ital.* **1995**, *125*, 181−188.
(16) Sanz, D.; Santa Maria, M. D.; Claramunt, R. M.; Cano, M.; Heras, J. V.; Campo, J. A.; Ruiz, F. A.; Pinilla, E.; Monge, A. *J. Organomet. Chem.* **1996**, 526, 341−350.
(17) Oldham, W. J. Ph.D. Thesis, University of Washington, Seattle, WA, 1996.
(18) Alvarado, Y.; Boutry, O.; Gutiérrez, E.; Monge, A.; Micasio, M. C.; Poveda, M. L.; Peréz, P. J.; Ruiz, C.; Bianchini, C.; Carmona, E. *Chem. Eur. J.* **1997**, *3*, 860−873.
(19) Albinati, A.; Bovens, M.; Rüegger, H.; Venazi, L. M. *Inorg. Chem.* **1997**, *36*, 5991−5999.
(20) Akita, M.; Ohta, K.; Takahashi, Y.; Hikichi, S.; Moro-oka, Y. *Organometallics* **1997**, *16*, 4121−4128.
(21) Keyes, M. C.; Young, V. G.; Tolman, W. B. *Organometallics* **1996**, *15*, 4133−4140.
(22) Ghosh, C. K. Ph.D. Thesis, University of Alberta, Edmonton, AB, Canada, 1988.
(23) Ghosh, C. K.; Rodgers, D. P. S.; Graham, W. A. G. *J. Chem. Soc., Chem. Commun.* **1988**, 1511−1512.
(24) Steyn, M. M. D.; Singleton, E.; Hietkamp, S.; Liles, D. C. *J. Chem. Soc., Dalton Trans.* **1990**, 2991−2997.
(25) Purwoko, A. A.; Lees, A. J. *Inorg. Chem.* **1996**, *35*, 675−682.
(26) Chauby, V.; Le Berre, S.; Kalck, P.; Daran, J.-C.; Commenges, G. *Inorg. Chem.* **1996**, *35*, 6354−6355.
(27) Connelly, N. G.; Emslie, D. J. H.; Metz, B.; Orpen, A. G.; Quayle, M. *J. Chem. Commun.* **1996**, 2289−2290.
(28) Oldham, W. J.; Heinekey, D. M. *Organometallics* **1997**, *16*, 467−474.
(29) Oldham, W. J.; Hinkle, A. S.; Heinekey, D. M. *J. Am. Chem. Soc.* **1997**, *119*, 11028−11036.

10.1021/om9805685 CCC: $15.00
Publication on Web 10/16/1998

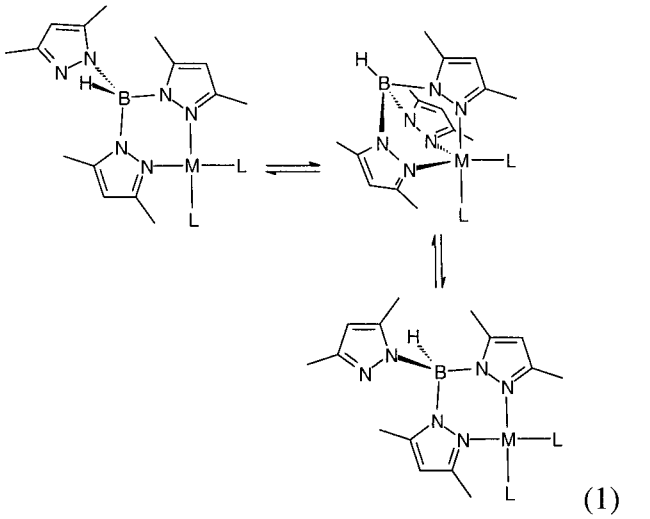

(1)

Recently Akita et al.[20] showed that the frequency of the B−H stretch in the infrared region could be used to determine the hapticity of the tris(pyrazolyl)borate ligands in complexes of the type Tp^RML_n, both in solution and in the solid state. An increase in the electron-donating ability of the substituents on the pyrazolyl ring resulted in a shift of the B−H stretching frequency to higher energy. When R = ^{i}Pr or Me, values for ν_{B-H} above 2500 cm^{-1} were indicative of η^3 coordination of the tris(pyrazolyl)borate, while values below 2500 cm^{-1} indicated that the ligand was bound in an η^2 fashion. In this work we wish to report that the ^{11}B NMR chemical shift of the tris(pyrazolyl)borate ligand can also be used to determine the coordination geometry at the metal center.[30]

Results and Discussion

Tp*Rh(CNCHMe$_2$)$_2$ (**1**) and Tp*Rh(CNCMe$_3$)$_2$ (**2**) were prepared by addition of 4 equiv of the appropriate isocyanide to a stirred benzene solution of [Rh(COE)$_2$Cl]$_2$ (COE = cyclooctene) followed by addition of KTp*. The ^{1}H and ^{13}C NMR spectra of **1** and **2** show resonances for only one type of pyrazolyl ring. IR spectra of **1** and **2** in THF contain absorptions at 2154 and 2101 cm^{-1} (**1**) and at 2144 and 2101 cm^{-1} (**2**). These absorptions are assigned to the symmetric and asymmetric stretches of the isocyanide ligands and are consistent with their coordination to Rh^I metal centers. Additionally, the IR spectra show bands assigned to the B−H stretch of **1** and **2** at 2468 and 2465 cm^{-1}, respectively. These values are consistent with η^2 coordination as observed by Akita. The ^{11}B{^{1}H} NMR spectra of **1** and **2** show a single resonance at δ −6.78 and −6.99, respectively. X-ray diffraction studies to determine the solid-state structure of **2** show a rotational disorder of the *tert*-butyl groups, resulting in poor refinement (see Supporting Information). However, the data unambiguously show that the tris(pyrazolyl)borate ligand in **2** is η^2-bound (Figure 1). This type of coordination is also observed in the structurally characterized bis(isocyanide) complexes Tp*Rh(CNCH$_2$CMe$_3$)$_2$ (**3**) and Tp*Rh(CN-2,6-xylyl)$_2$ (**4**).[8]

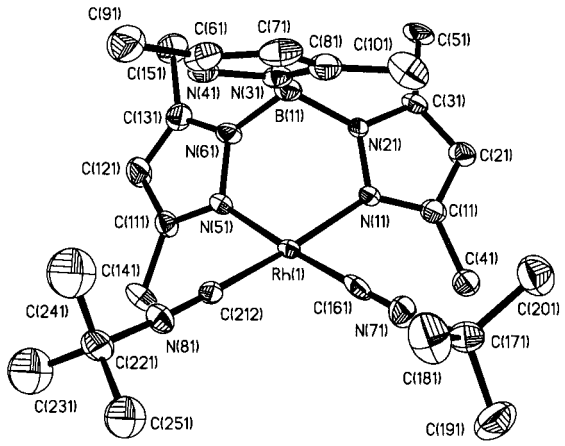

Figure 1. ORTEP drawing of Tp*Rh(CNCMe$_3$)$_2$ (**2**). Ellipsoids are shown at the 30% probability level. Hydrogen atoms have been omitted for clarity. Selected distances (Å): Rh1−C161, 1.874(14); Rh1−C212, 1.879(10); Rh1−N51, 2.069(9); Rh1−N11, 2.092(8).

When Tp*Rh(CNCH$_2$CMe$_3$)$_2$ (**3**) is dissolved in dichloromethane, the bright yellow solution loses color over the course of 2 h, resulting in the formation of [Tp*Rh(CNCH$_2$CMe$_3$)$_2$(CH$_2$Cl)]Cl (**18**) in good yield. Isolated as a white air-stable solid, the ^{1}H NMR spectrum of **18** shows 6 pyrazolyl resonances in a 2:1 (4 pz *Me* resonances and 2 pz *H* resonances) ratio, indicating the equivalence of two of the three pyrazolyl rings. Resonances for the neopentyl methyl and methylene protons appear at δ 1.15 and 3.80, integrated to 18 and 4 protons, respectively. The methylene protons of the activated dichloromethane molecule are diastereotopic and appear as two doublets of doublets at δ 5.26 and 5.14. Due to the poor solubility of **18** in THF IR data were obtained in CH_2Cl_2. Absorptions at 2165 and 2108 cm^{-1} are assigned to the symmetric and asymmetric stretches of the two isocyanide ligands. The B−H stretch of **18** is observed at 2522 cm^{-1}, indicating η^3 coordination of the pyrazolylborate ligand. A single peak in the ^{11}B{^{1}H} NMR spectrum appears at δ −9.76. The solid-state structure of **18** was determined by X-ray crystallography (Figure 2) and supports the structural conclusions made from the spectroscopic data.

To examine the relationship between the ^{11}B NMR chemical shift and the hapticity of the pyrazolylborate ligand, a number of Tp*ML$_n$ complexes were prepared according to published literature procedures (**5**−**17**, **19**−**23**). When possible, structurally characterized examples were chosen. All IR and ^{11}B NMR data were obtained in THF, with the exception of **18**, to minimize possible reaction with solvent. The B−H stretching frequency was independent of solvent, with less than a 2 cm^{-1} difference observed in a variety of solvents for most compounds. The data are summarized in Table 1.

The ^{11}B{^{1}H} NMR spectra of **1**−**23** in THF show resonances in the region from δ −5.90 to −9.76. The peaks are broad and featureless but exhibit a remarkable trend: the chemical shift of the boron nucleus shows an excellent correlation with the hapticity of the tris(pyrazolyl)borate ligand. All η^2-pyrazolylborate complexes presented in this work show resonances between δ −5.90 and −6.99, while resonances for complexes

(30) For ^{11}B NMR spectra of other transition-metal complexes, see: (a) Stainer, M. V. R.; Takats, J. *J. Am. Chem. Soc.* **1983**, *105*, 410−415. (b) Marques, N.; De Matos, A. P.; Bagnall, K. W. *Inorg. Chim. Acta* **1984**, *95*, 75−77. (c) Bucher, U. E.; Currao, A.; Nesper, R.; Rüegger, H.; Venanzi, L. M.; Younger, E. *Inorg. Chem.* **1995**, *34*, 66−74.

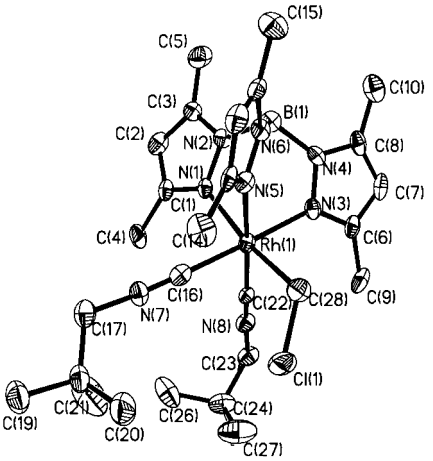

Figure 2. ORTEP drawing of [Tp*Rh(CNCH$_2$CMe$_3$)$_2$(CH$_2$-Cl)]Cl (**18**). Ellipsoids are shown at the 50% probability level. Hydrogen atoms have been omitted for clarity. Selected distances (Å): Rh1−C16, 1.949(8); Rh1−C22, 1.962(8); Rh1−C28, 2.069(7); Rh1−N1, 2.161(5); Rh1−N3, 2.082(5); Rh1−N5, 2.077(5).

Table 1. B−H Stretching Frequency, ^{11}B Chemical Shift, and Hapticity for Tp*ML$_n$ Complexes

complex	ν_{B-H} (cm^{-1})[a]	^{11}B (δ)[a]	hapticity
Rh^{I} Compounds			
Tp*Rh(CNCHMe$_2$)$_2$ (**1**)	2468	−6.78	2
Tp*Rh(CNCMe$_3$)$_2$ (**2**)	2465	−6.99	2[b]
Tp*Rh(CNCH$_2$CMe$_3$)$_2$ (**3**)	2467	−5.90	2[b]
Tp*Rh(CN-2,6-xylyl)$_2$ (**4**)	2467	−6.59	2[b]
Tp*Rh(CO)(PMe$_3$) (**5**)	2471	−6.35	2[b]
Tp*Rh(C$_2$H$_4$)(CNCH$_2$CMe$_3$) (**6**)	2523	−9.38	3
Tp*Rh(C$_2$H$_4$)(CN-2,6-xylyl) (**7**)	2525	−9.28	3[b]
Tp*Rh(C$_2$H$_4$)$_2$ (**8**)	2525	−9.17	3
Tp*Rh(C$_2$H$_3$CH$_3$)(CNCH$_2$CMe$_3$) (**9**)	2523	−9.13	3
Tp*Rh(CO)$_2$ (**10**)	2524	−9.25	3
Tp*Rh(CO)(C$_2$H$_4$) (**11**)	2521	−9.37	3
Tp*Rh(CNCH$_2$CMe$_3$)-(PhN=C=N CH$_2$CMe$_3$) (**12**)	2525	−9.71	3
Rh^{III} Compounds			
Tp*Rh(CNCH$_2$CMe$_3$)Cl$_2$ (**13**)	2533	−9.36	3
Tp*Rh(PMe$_3$)Cl$_2$ (**14**)	2535	−9.64	3[b]
Tp*Rh(CNCH$_2$CMe$_3$)(H)$_2$ (**15**)	2524	−9.26	3
Tp*Rh(CNCH$_2$CMe$_3$)(Me)Cl (**16**)	2529	−9.28	3
Tp*Rh(CNCH$_2$CMe$_3$)(CHCH$_2$)(Cl) (**17**)	2529	−9.10	3
[Tp*Rh(CNCH$_2$CMe$_3$)$_2$(CH$_2$Cl)]Cl (**18**)	2522[c]	−9.76	3[b]
Ir Compounds			
Tp*Ir(COD) (**19**)	2476	−6.47	2[b]
Tp*Ir(C$_2$H$_4$)$_2$ (**20**)	2533	−8.74	3[b]
Tp*Ir(C$_2$H$_4$)(C$_2$H$_3$)H (**21**)	2527	−8.76	3
Pt Compounds			
PPN[Tp*Pt(Me)$_2$] (**22**)	2458	−6.44	2[b]
Tp*Pt(C$_6$H$_5$)$_2$H (**23**)	2531	−8.44	3

[a] Recorded in THF. [b] Characterized by X-ray crystallography. [c] Recorded in CH_2Cl_2.

containing η^3-pyrazolylborate ligands appear between δ −8.44 and −9.76. A plot of B−H stretching frequency versus ^{11}B chemical shift clearly demonstrates this trend (Figure 3). The data for **1**−**23** suggest that the trend in ^{11}B chemical shift is independent of charge and is general for group 9 and 10 metals, as Rh^{I} vs Rh^{III}, Ir^{I} vs Ir^{III}, and Pt^{II} vs Pt^{IV} species fall distinctly within the two regions.

In only one instance does our data suggest a binding mode different from the hapticity assignment previously made in the literature. Tp*Rh(CO)(C$_2$H$_4$) (**11**) was identified as a 16-electron square-planar complex con-

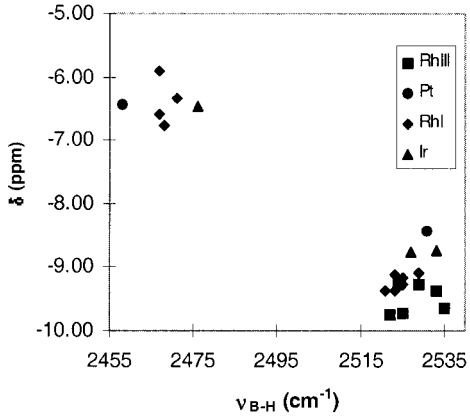

Figure 3. Plot of ν_{B-H} versus ^{11}B chemical shift showing the correlation between stretching frequency, chemical shift, and hapticity.

taining an η^2-tris(pyrazolyl)borate ligand.[23] This determination was based solely on the very minor difference in carbonyl stretching frequency observed between **11** and the bis(pyrazolyl)borate analogue—which is by necessity η^2. However, both the B−H stretching frequency and the ^{11}B NMR chemical shift suggest that the pyrazolylborate ligand is η^3-bound in solution. Trigonal-bipyramidal geometry is observed in the similar, structurally characterized complexes Tp*Rh(CN-2,6-xylyl)(C$_2$H$_4$) (**7**)[31] and Tp*Ir(PPhMe$_2$)(C$_2$H$_4$).[32] We therefore assign **11** as possessing trigonal-bipyramidal geometry with the pyrazolylborate ligand coordinated in an η^3 fashion rather than the η^2 mode previously reported.

The question of why the ^{11}B NMR chemical shift can be used to determine the hapticity of the ligand remains to be answered. There appears to be no direct relationship between the average N−B−N angle or average N−B bond length and the chemical shift of the boron nucleus in complexes for which X-ray data are available (Table 2). This effectively rules out small changes in hybridization at boron as the source of the differences in chemical shift. It should be noted that in structurally characterized η^2-Tp*ML$_n$ complexes the uncoordinated pyrazolyl ring lies parallel to the square plane of the metal rather than "perpendicular" as is seen in trigonal-bipyramidal structures. A simple inductive effect due to coordination of the third ring to the metal center or a ring current effect associated with this change in geometry cannot be ruled out.

In summary, a series of Tp*ML$_n$ complexes have been prepared and characterized. Analysis of the infrared and ^{11}B NMR data for these complexes shows a strong correlation between the chemical shift of the boron nucleus, the frequency of the B−H stretch, and the hapticity of the tris(pyrazolyl)borate ligand. The correlation between chemical shift and hapticity is independent of the charge of the metal center and is general for group 9 and 10 metals. Though only tris(3,5-dimethylpyrazolyl)borate complexes were examined in this study, it is likely that the use of ^{11}B NMR chemical shifts for the determination of hapticity will be a general

(31) Wick, D. D.; Northcutt, T. O.; Lachicotte, R. J.; Jones, W. D. *Organometallics* **1998**, *17*, 4484−4492.
(32) Gutiérrez-Puebla, E.; Monge, A; Nicasio, M. C.; Pérez, P. J.; Poveda, M. L.; Rey, L.; Ruíz, C.; Carmona, E. *Inorg. Chem.* **1998**, *37*, 4538−4546.

Table 2. Average Bond Distances and Angles for Selected Tris(pyrazolyl)borate Complexes

complex	hapticity	av N−B−N angle (deg)	av B−N distance (Å)	^{11}B (δ)
Tp*Rh(C_2H_4)(CN-2,6-xylyl) (**7**)	η^3	108.1	1.551	−9.28
[Tp*Rh($CNCH_2CMe_3$)$_2$(CH_2Cl)]Cl (**18**)	η^3	109.0	1.539	−9.76
Tp*Rh(CO)(PMe_3) (**5**)	η^2	109.2	1.547	−6.35
Tp*Rh($CNCH_2CMe_3$)$_2$ (**3**)	η^2	109.7	1.544	−5.90
Tp*Rh(CN-2,6-xylyl)$_2$ (**4**)	η^2	110.3	1.537	−6.59
Tp*Rh(PMe_3)Cl_2 (**14**)	η^3	110.7	1.532	−9.64
PPN[Tp*PtMe_2] (**22**)	η^2	112.1	1.541	−6.44

trend for a variety of poly(pyrazolyl)borate complexes, much as the trend in B−H stretching frequency was observed to be general for a variety of Tp^R complexes. ^{11}B NMR spectra are easily acquired, making this an attractive method for the rapid determination of the solution-state structure of tris(pyrazolyl)borate metal complexes.

Experimental Section

General Considerations. All reactions, recrystallizations, chromatography, and routine manipulations, unless otherwise noted, were carried out at ambient temperature under a nitrogen atmosphere, either on a high-vacuum line using modified Schlenk techniques or in a Vacuum Atmospheres Corp. Dri-lab. All aromatic and hydrocarbon solvents were distilled under nitrogen or vacuum from dark purple solutions of sodium benzophenone ketyl. Chlorinated solvents were distilled under vacuum from calcium hydride suspensions. Tp*Rh(CO)(PMe_3),[22] Tp*Rh(C_2H_4)($CNCH_2CMe_3$),[31] Tp*Rh(C_2H_4)(CN-2,6-xylyl),[31] Tp*Rh($C_2H_3CH_3$)($CNCH_2CMe_3$),[31] Tp*Rh(CO)$_2$,[6] Tp*Rh(CO)(C_2H_4),[23] Tp*Rh($CNCH_2CMe_3$)Cl_2,[33] Tp*Rh(PMe_3)Cl_2,[34] Tp*Rh($CNCH_2CMe_3$)(H)$_2$,[34] Tp*Rh($CNCH_2CMe_3$)(Me)Cl,[33] Tp*Rh($CNCH_2CMe_3$)($CHCH_2$)(Cl),[33] Tp*Ir(COD),[19] Tp*Ir(C_2H_4)$_2$,[18] Tp*Rh($CNCH_2CMe_3$)(PhN=C=NCH_2CMe_3),[35] and Tp*Rh(C_2H_4)$_2$[3] were prepared as described in the literature. Improved syntheses for Tp*Rh($CNCH_2CMe_3$)$_2$ and Tp*Rh(CN-2,6-xylyl)$_2$ are presented.[8]

^{1}H (400 MHz), ^{13}C (100 MHz), and ^{11}B (128 MHz) NMR spectra were recorded on a Bruker AMX-400 spectrometer. All ^{1}H NMR chemical shifts are reported in ppm (δ) relative to tetramethylsilane and referenced to the chemical shifts of residual solvent resonances (C_6D_6, δ 7.15; d_8-THF, δ 1.73; CD_2Cl_2, δ 5.32). Chemical shifts for ^{13}C NMR were measured in ppm relative to the deuterated solvent resonance (C_6D_6, δ 128.0; CD_2Cl_2, δ 53.8). Chemical shifts for ^{11}B NMR were measured in ppm relative to external BF_3·OEt_2 (sealed capillary) in d_8-THF. ^{11}B NMR spectra were acquired in d_8-THF using an 8 μs pulse width, 10 ms delay, and 50 ms acquisition time. Elemental analyses were performed by Desert Analytics. A Siemens SMART (CCD) diffractometer was used for X-ray crystal structure determination of complex **18**. Infrared spectra were recorded by a Mattson Instruments 6020 Galaxy Series FTIR and processed with First:Aquire v1.52 software.

Synthesis of Tp*Rh($CNCHMe_2$)$_2$ (1). A 50 mL round-bottom flask containing a Teflon-coated stir bar was charged with 215 mg (0.300 mmol) of [$(COE)_2RhCl]_2$. Addition of 20 mL of benzene resulted in an orange solution. To the stirred solution was added 95 mg (1.37 mmol, 4.5 equiv) of isopropyl isocyanide. The resulting purple solution was stirred for 2 h. KTp* (210 mg, 0.630 mmol, 2.1 equiv) was added in one portion and the solution stirred for 2 h. Insoluble materials were removed by filtration, and the yellow filtrate was evaporated to dryness. Recrystallization from toluene−hexanes at −20 °C gave 310 mg (0.576 mmol, 96%) as bright yellow plates. ^{1}H NMR (C_6D_6): δ 5.85 (s, 3H, pz *H*), 3.05 (sept, J_{HH} = 6.4 Hz, 2H, C*H*(CH_3)$_2$), 2.50 (s, 9H, pz CH_3), 2.28 (s, 9H, pz CH_3), 0.77 (d, J_{HH} = 6.4 Hz, 12H, CH(CH_3)$_2$). ^{13}C{^{1}H} NMR (C_6D_6): δ 150.89 (d, J_{RhH} = 65.3 Hz, *CN*CH(CH_3)$_2$), 148.39 (s, pz), 144.45 (s, pz), 105.57 (s, pz), 47.61 (s, *C*H(CH_3)$_2$), 23.28 (s, CH(*C*H_3)$_2$), 15.58 (s, pz *C*H_3), 13.05 (s, pz *C*H_3). ^{11}B{^{1}H} NMR (d_8-THF): δ −6.78 (bs). IR (THF, cm^{-1}): 2467 (w, B−H), 2154 (s, CNR), 2101 (s, CNR). Anal. Calcd (found) for $C_{23}H_{36}N_8BRh$: C, 51.32 (51.25); H, 6.58 (6.74); N, 20.81 (20.54).

Synthesis of Tp*Rh($CNCMe_3$)$_2$ (2). To a stirred benzene solution of [$(CNCMe_3)_2RhCl]_2$ (177 mg, 0.291 mmol) was added 42 mg (0.582 mmol, 2 equiv) of KTp*. The solution was stirred overnight. The yellow solution was filtered to remove insolubles and the filtrate evaporated to dryness, yielding a yellow solid. Recrystallization from toluene-hexanes at −20 °C gave 280 mg (0.503 mmol, 86%) as bright yellow-green microcrystals. ^{1}H NMR (C_6D_6): δ 5.82 (s, 3H, pz *H*), 2.51 (s, 9H, pz CH_3), 2.26 (s, 9H, pz CH_3), 0.99 (s, 18H, C(CH_3)$_3$). ^{13}C-{^{1}H} NMR (C_6D_6): δ 148.38 (J_{RhC} = 66 Hz, *C*NR), 145.77 (s, pz), 141.78 (s, pz), 102.90 (s, pz), 53.10 (s, CN*C*(CH_3)$_3$), 28.01 (s, CNC(*C*H_3)$_3$), 13.05 (s, pz *C*H_3), 10.48 (s, pz *C*H_3). ^{11}B{^{1}H} NMR (d_8-THF): δ −6.99 (bs). IR (THF, cm^{-1}): 2464 (w, B−H), 2144 (s, CNR), 2102 (s, CNR). Anal. Calcd (found) for $C_{25}H_{40}N_8BRh$: C, 52.55 (52.84); H, 7.06 (7.05); N, 19.61 (19.81).

Synthesis of Tp*Rh($CNCH_2CMe_3$)$_2$ (3). This procedure is a modification of a previously reported synthesis, which employed [$(C_2H_4)_2RhCl]_2$.[8] A 50 mL round-bottom flask containing a Teflon-coated stir bar was charged with 218 mg (0.304 mmol) of [$(COE)_2RhCl]_2$. Addition of 15 mL of benzene resulted in an orange suspension. To the stirred suspension was added 153 μL (1.28 mmol, 4.2 equiv) of neopentyl isocyanide. The resulting orange solution was stirred for 2 h. KTp* (250 mg, 0.746 mmol, 2.4 equiv) was added in one portion and the solution stirred for 2 h. Insoluble materials were removed by filtration, and the bright orange filtrate was evaporated to dryness. Recrystallization from hexanes at −20 °C gave 345 mg (0.583 mmol, 96%) as yellow-orange microcrystals. ^{11}B-{^{1}H} NMR (d_8-THF): δ −5.90 (bs). IR (THF, cm^{-1}): 2467 (w, B−H), 2161 (s, CNR), 2108 (s, CNR).

Synthesis of Tp*Rh(CN-2,6-xylyl)$_2$ (4). This procedure is a modification of a previously reported synthesis, which employed [$(C_2H_4)_2RhCl]_2$.[8] A 50 mL round-bottom flask containing a Teflon-coated stir bar was charged with 228 mg (0.317 mmol) of [$(COE)_2RhCl]_2$. Addition of 10 mL of benzene resulted in an orange suspension. To the stirred suspension was added 167 mg (1.27 mmol, 4.1 equiv) of 2,6-xylyl isocyanide. The solution was stirred for 2 h. KTp* (240 mg, 0.716 mmol, 2.25 equiv) was added in one portion and the solution stirred for 2 h. Insoluble materials were removed by filtration, and the bright orange filtrate was evaporated to dryness. Recrystallization from hexanes at −20 °C gave 373 mg (0.563 mmol, 89%) as yellow-orange microcrystals. ^{11}B{^{1}H} NMR (d_8-THF): δ −6.59 (bs). IR (THF, cm^{-1}): 2467 (w, B−H), 2129 (s, CNR), 2063 (s, CNR).

Synthesis of [Tp*Rh($CNCH_2CMe_3$)$_2$(CH_2Cl)]Cl (18). In a 25 mL round-bottom flask containing a Teflon-coated stir bar 45 mg (0.076 mmol) Tp*Rh($CNCH_2CMe_3$)$_2$ was dissolved in 10 mL of CH_2Cl_2. The bright yellow solution fades over 2 h of stirring, yielding a pale yellow solution. The solvent was removed in vacuo and the crude product dissolved in benzene. A white solid was isolated by filtration. Recrystallization from

(33) Wick, D. D.; Jones, W. D. *Inorg. Chem.* **1997**, *36*, 2723−2729.
(34) Wick, D. D. Ph.D. Thesis, University of Rochester, Rochester, NY, 1996.
(35) Hessell, E. T.; Jones, W. D. *Organometallics* **1992**, *11*, 1496−1505.

Table 3. Selected Crystallographic Data for [Tp*Rh(CNCH$_2$CMe$_3$)$_2$(CH$_2$Cl)]Cl and Tp*Rh(CNCMe$_3$)$_2$

	[Tp*Rh(CNCH$_2$CMe$_3$)$_2$-(CH$_2$Cl)]Cl·2CH$_2$Cl$_2$	Tp*Rh(CNCMe$_3$)$_2$
chem formula	$C_{30}H_{50}BCl_6N_8Rh$	$C_{25}H_{40}BN_8Rh$
fw	849.20	566.37
cryst syst	monoclinic	monoclinic
space group (No.), Z	$C2/c$ (15), 8	$P2_1/n$ (14), 8
a, Å	17.1078(3)	20.4876(4)
b, Å	20.7753(1)	15.4819(1)
c, Å	22.3941(4)	20.6470(3)
β, deg	91.02(1)	105.50(10)
V, Å^3	7958.0(2)	6095.4(2)
ρ_{calcd}, g cm^{-3}	1.418	1.234
temp, °C	−80	−80
no. of data collected	15 816	25 681
no. of unique data	5550	8496
no. of params varied	431	599
R1(F_o), wR2(F_o^2), ($I > 2\sigma(I)$)	0.0691, 0.1581	0.0917, 0.2125
R1(F_o), wR2(F_o^2), all data	0.0995, 0.1742	0.1002, 0.2160
goodness of fit	1.071	1.268

CH_2Cl_2−hexanes at −20 °C gave 36 mg (0.053 mmol, 70%) as colorless crystals. ^{1}H NMR (CD_2Cl_2): δ 5.99 (s, 2H, pz *H*), 5.93 (s, 1H, pz *H*), 5.26 (dd, J_{HH} = 6.8 Hz, J_{RhH} = 3.1 Hz, C*H*HCl), 5.14 (dd, J_{HH} = 6.8 Hz, J_{RhH} = 2.1 Hz, CH*H*Cl), 3.80 (bd, J_{HH} = 2.4 Hz, 4H, C*H*$_2$C(CH$_3$)$_3$), 2.52 (s, 6H, pz C*H*$_3$), 2.39 (s, 6H, pz C*H*$_3$), 2.37 (s, 3H, pz C*H*$_3$), 2.29 (s, 3H, pz C*H*$_3$), 1.15 (s, 18H, CH$_2$C(C*H*$_3$)$_3$). ^{13}C{^{1}H} NMR (CD_2Cl_2): δ 150.71, 149.56, 145.63, 156.15 (s, pz), 126.80 (bm, *C*NR), 108.15, 106.51 (pz), 51.54 (s, CN*C*H$_2$C(CH$_3$)$_3$), 34.631 (d, J_{RhC} = 21.5 Hz, *C*H$_2$Cl), 32.00 (s, CNCH$_2$*C*(CH$_3$)$_3$), 26.27 (s, CNCH$_2$C(*C*H$_3$)$_3$), 14.06, 12.12, 11.73 (s, pz *C*H$_3$). ^{11}B{^{1}H} NMR (d_8-THF): δ −9.76 (bs). IR (CH_2Cl_2, cm^{-1}): 2522 (w, B−H), 2165 (s, CNR), 2108 (s, CNR). Anal. Calcd (found) for $C_{28}H_{46}N_8BCl_2Rh·3CH_2Cl_2$: C, 39.64 (39.77); H, 5.56 (5.81); N, 11.93 (12.31).

X-ray Structural Determination of [Tp*Rh(CNCH$_2$-CMe$_3$)$_2$(CH$_2$Cl)]Cl. A colorless crystal of approximate dimensions 0.20 × 0.16 × 0.04 mm^3 was mounted under Paratone-8277 on a glass fiber and immediately placed under a cold nitrogen stream at −80 °C on the X-ray diffractometer. The X-ray intensity data were collected on a standard Siemens SMART CCD area detector system equipped with a normal-focus molybdenum-target X-ray tube operated at 2.0 kW (50 kV, 40 mA). A total of 1321 frames of data (1.3 hemispheres) were collected using a narrow-frame method with scan widths of 0.3° in ω and exposure times of 60 s/frame using a detector-to-crystal distance of 5.09 cm (maximum 2θ angle of 56.6°). The total data collection time was approximately 26 h. Frames were integrated to a maximum 2θ angle of 46.6° with the Siemens SAINT program to yield a total of 15 816 reflections, of which 5550 were independent (R_{int} = 5.98%, R_{sig} = 6.95%)[36] and 4159 were above 2σ(I). Laue symmetry revealed a monoclinic crystal system, and the final unit cell parameters (at −80 °C) were determined from the least-squares refinement of three-dimensional centroids of 7515 reflections.[37] Data were corrected for absorption with the SADABS[38] program.

The space group was assigned as $C2/c$, and the structure was solved by using direct methods and refined employing full-matrix least-squares on F^2 (Siemens, SHELXTL,[39] version 5.04). For a Z value of 8, there is one molecule, one chloride anion, and two methylene chlorides in the asymmetric unit. All of the non-H atoms were refined anisotropically, and the hydrogen atoms were included in idealized positions. The structure was refined to a goodness of fit (GOF) of 1.071 and final residuals[40] of R1 = 6.91% ($I > 2\sigma(I)$) and wR2 = 15.81% ($I > 2\sigma(I)$). Selected crystallographic data are given in Table 3.

X-ray Structural Determination of Tp*Rh(CNCMe$_3$)$_2$. A yellow crystal of approximate dimensions 0.38 × 0.24 × 0.14 mm^3 was mounted under Paratone-8277 on a glass fiber and immediately placed in a cold nitrogen stream at −80 °C on the X-ray diffractometer. The X-ray intensity data were collected on a standard Siemens SMART CCD area detector system equipped with a normal-focus molybdenum-target X-ray tube operated at 2.0 kW (50 kV, 40 mA). A total of 1321 frames of data (1.3 hemispheres) were collected using a narrow-frame method with scan widths of 0.3° in ω and exposure times of 30 s/frame using a detector-to-crystal distance of 5.09 cm (maximum 2θ angle of 56.6°). The total data collection time was approximately 12 h. Frames were integrated to a maximum 2θ angle of 46.5° with the Siemens SAINT program to yield a total of 25 681 reflections, of which 8496 were independent (R_{int} = 3.77%, R_{sig} = 4.13%)[36] and 7350 were above 2σ(I). Laue symmetry revealed a monoclinic crystal system, and the final unit cell parameters (at −80 °C) were determined from the least-squares refinement of three-dimensional centroids of 8192 reflections.[37] Data were corrected for absorption with the SADABS[38] program.

The space group was assigned as $P2_1/n$, and the structure was solved by using direct methods and refined employing full-matrix least-squares on F^2 (Siemens, SHELXTL,[39] version 5.04). For a Z value of 8, there are two independent molecules in the asymmetric unit. One of the *t*-Bu groups was disordered, and the occupancies of the disordered atoms were refined to a 60:40 ratio. Nearly all other non-H atoms were refined anisotropically, and the hydrogen atoms were included in idealized positions. The structure was refined to a goodness of fit (GOF) of 1.268 and final residuals[40] of R1 = 9.17% ($I > 2\sigma(I)$), and wR2 = 21.25% ($I > 2\sigma(I)$). Selected crystallographic data are given in Table 3.

Acknowledgment is made to the U.S. Department of Energy (Grant FG02-86ER13569) for their support of this work. We thank Dr. D. Wick and Prof. K. Goldberg for the generous donation of Tp*Pt(C$_6$H$_5$)$_2$H and PPN[Tp*Pt(Me)$_2$].[41]

Supporting Information Available: Tables of crystallographic data, coordinates, thermal parameters, and bond distances and angles for **2** and **18** (14 pages). Ordering information is given on any masthead page.

OM9805685

(36) $R_{int} = \sum|F_o^2 - F_o^2(mean)|/\sum[F_o^2]$; $R_{sigma} = \sum[\sigma(F_o^2)]/\sum[F_o^2]$.

(37) It has been noted that the integration program SAINT produces cell constant errors that are unreasonably small, since systematic error is not included. More reasonable errors might be estimated at 10× the listed value.

(38) The SADABS program is based on the method of Blessing; see: Blessing, R. H. *Acta Crystallogr., Sect A* **1995**, *51*, 33.

(39) SHELXTL: Structure Analysis Program, version 5.04; Siemens Industrial Automation Inc.: Madison, WI, 1995.

(40) GOF = $[\sum[w(F_o^2 - F_c^2)^2]/(n - p)]^{1/2}$, where n and p denote the number of data and parameters. R1 = $(\sum||F_o| - |F_c||)/\sum|F_o|$; wR2 = $[\sum[w(F_o^2 - F_c^2)^2]/\sum[w(F_o^2)^2]]^{1/2}$, where $w = 1/[\sigma^2(F_o^2) + (aP)^2 + bP]$ and $P = [(Max;0,F_o^2) + 2F_c^2]/3$.

(41) (a) Wick, D. D.; Goldberg, K. I. *J. Am. Chem. Soc.* **1997**, *119*, 10235−10236. (b) O'Reilly, S. A.; White, P. S.; Templeton, J. L. *J. Am. Chem. Soc.* **1996**, *118*, 5684−5689.